J|A|C|S
ARTICLES
Published on Web 07/20/2004

Ab Initio Molecular Dynamics Simulations and g-Tensor Calculations of Aqueous Benzosemiquinone Radical Anion: Effects of Regular and "T-Stacked" Hydrogen Bonds

James R. Asher,[†] Nikos L. Doltsinis,[‡] and Martin Kaupp*,[†]

Contribution from the Institut für Anorganische Chemie, Universität Würzburg, Am Hubland, D-97074 Würzburg, Germany and Lehrstuhl für Theoretische Chemie, Ruhr-Universität Bochum, D-44780 Bochum, Germany

Received March 15, 2004; E-mail: kaupp@mail.uni-wuerzburg.de

Abstract: Car−Parrinello molecular dynamics (CP-MD) simulations of the benzosemiquinone radical anion in aqueous solution have been performed at ambient conditions. Analysis of the trajectory shows not only extensive hydrogen bonding to the carbonyl oxygen atoms (ca. 4−5.6 water molecules depending on distance criteria), but also relatively long-lived "T-stacked" hydrogen bonds to the semiquinone π-system. These results are discussed in the context of recent findings on semiquinone-protein interactions in photosynthetic reaction centers, and of EPR and vibration spectroscopical data for the aqueous system. Snapshots from the CP-MD trajectory are used for the first quantum chemical analyses of dynamical effects on electronic g-tensors, using cluster models and a recently developed density functional method. In particular, the effects of intermolecular hydrogen-bond dynamics on the g-tensor components are examined, in comparison with recent EPR and ENDOR studies.

1. Introduction

Quinones and their reduced forms, semiquinones and dihydroquinones, are of considerable biological interest, as they occur in all living beings as antioxidants and as redox couples for electron transfer in respiration and photosynthesis.[1] EPR spectroscopy is one of the central methods for probing the environment of semiquinone radical anions and other paramagnetic species, both in their protein environments and in other media.[2] In particular, the recent development of high-field EPR methods has provided access to the important anisotropy of the electronic g-tensor of bioradicals such as semiquinones.[3] The g-tensor is a sensitive probe of intermolecular interactions between the protein environment and the radical of interest.

Using a recently developed density functional theory (DFT) approach,[4] unprecedented accuracy in the calculation of electronic g-tensors for various bioradicals such as semiquinones,[5−8] tyrosyl radicals,[4,9] or nitroxides,[10] has been demonstrated. In particular, the important semiquinones have been studied in detail by DFT methods, both in isotropic solution[5,7,11,12] and in the protein environment of various photosynthetic reaction centers.[6,8] A notable result has been the identification of T-stacked hydrogen bonds from a nearby tryptophan residue to the semiquinone in variants of photosystem I (PS−I),[8] in which the native phylloquinone had been reconstituted by smaller quinones.[13] The computational study, which involved the direct comparison of calculated and measured g-tensors, suggested that such T-stacked hydrogen bonding may be a general feature of tryptophan/semiquinone interactions, with potential consequences for the redox potential of quinone/semiquinone redox couples in biology.[8]

Quantum chemical g-tensor calculations may thus provide important insights into structure and mechanistic details of biological redox processes and greatly increase the amount of information that may be extracted from multi-frequency EPR spectra. Until now, all quantum chemical studies in this field

[†] Institut für Anorganische Chemie, Universität Würzburg.
[‡] Lehrstuhl für Theoretische Chemie, Ruhr-Universität Bochum.

(1) Patai, S. *Chemistry of Quinoid Compounds*; Interscience: New York, 1974. Trumpower, B. L., Ed. *Function of Quinones in Energy Conserving Systems*; Academic Press: New York, 1982. Morton, R. A. *Biochemistry of Quinones*; Academic Press: New York, 1965. *Coenzyme Q: Biochemistry, Bioenergetics, and Clinical Applications of Ubiquinone*; Lenaz, G., Ed.; John Wiley & Sons: Suffolk, 1985.
(2) Pedersen, J. A. *EPR Spectra from Natural and Synthetic Quinones and Quinoids*; CRC Press: Boca Raton, FL, 1985.
(3) For reviews see, e.g.: Lubitz, W.; Feher, G. *Appl. Magn. Reson.* **1999**, *17*, 1. Levanon, H.; Möbius, K. *Annu. Rev. Biophys. Biomol. Struct.* **1997**, *26*, 495.
(4) (a) Malkina, O. L.; Vaara, J.; Schimmelpfennig, B.; Munzarova, M.; Malkin, V. G.; Kaupp, M. *J. Am. Chem. Soc.* **2000,** *122*, 9206. (b) Kaupp, M.; Reviakine, R.; Malkina, O. L.; Arbuznikov, A.; Schimmelpfennig, B.; Malkin, V. G. *J. Comput. Chem.* **2002**, *23*, 794.
(5) Kaupp, M.; Remenyi, C.; Vaara, J.; Malkina, O. L.; Malkin, V. G. *J. Am. Chem. Soc.* **2002**, *124*, 2709.
(6) Kacprzak, S.; Kaupp, M. *J. Phys. Chem. B* **2004**, *108*, 2464.
(7) Ciofini, I.; Reviakine, R.; Arbuznikov, A.; Kaupp, M. *Theor. Chem. Acc.* **2004**, *111*, 132.
(8) Kaupp, M. *Biochemistry* **2002**, *41*, 2895.
(9) Kaupp, M.; Gress, T.; Reviakine, R.; Malkina, O. L.; Malkin, V. G. *J. Phys. Chem. B* **2003**, *107*, 331.
(10) Owenius, R.; Engström, M.; Lindgren, M.; Huber, M. *J. Phys. Chem. A* **2001**, *105*, 10 967. Engström, M.; Owenius, R.; Vahtras, O. *Chem. Phys. Lett.* **2001**, *338*, 407. Engström, M.; Vaara, J.; Schimmelpfennig, B.; Ågren, H. *J. Phys. Chem. B* **2002**, *106*, 12 354.
(11) Sinnecker, S.; Reijerse, E.; Neese, F.; Lubitz, W. *J. Am. Chem. Soc.* **2004**, *126*, 3280.
(12) See also: Neyman, K. M.; Ganyushin, D. I.; Rinkevičius, Ž.; Rösch, N. *Int. J. Quantum Chem.* **2002**, *90*, 1404.
(13) van der Est, A.; Sieckmann, I.; Lubitz, W.; Stehlik, D. *Chem. Phys.* **1995**, *194*, 349. Sieckmann, I.; van der Est, A.; Bottin, H.; Sétif, P.; Stehlik, D. *FEBS Lett.* **1991**, *284*, 98.

10.1021/ja0485053 CCC: $27.50

have relied on static structural data, which were either optimized computationally or taken from X-ray crystallography. However, dynamical effects—vibrational and conformational motion, and particularly the effects of breaking and forming of hydrogen bonds (or dynamical effects related to other intermolecular interactions)—cannot be accounted for using this method. Their inclusion into theoretical studies requires the carrying out of molecular dynamics (MD) simulations. There have been a number of classical force-field MD studies on quinones and semiquinones, both in aqueous solution[14−16] and in protein environments of photosynthetic reaction centers,[17] but in none of these were dynamical effects on EPR parameters studied. Although comparison of classical and ab initio molecular dynamics simulations on a gaseous ubisemiquinone model suggests a reasonable description of the side-chain conformation by the force field employed,[15] it is much less clear how well a classical force field simulates hydrogen bonding to a semiquinone radical anion. For example, the average hydrogen bond distances to the semiquinone oxygen atoms in a recent classical MD study of aqueous benzosemiquinone are 1.6 Å,[16] which is unrealistically short in comparison with quantum chemically optimized structures.[5,6,7,11] Similarly, it remains to be shown to what extent classical force fields properly reproduce T-stacked H-bonding to the π-system, whereas we found DFT calculations to be in excellent agreement with MP2 results for representative T-stacked complexes.[18] A faithful dynamical description of hydrogen bonding will be essential in describing not only EPR parameters but also the important redox properties of quinone/semiquinone redox couples.

We have therefore decided to perform extensive ab initio molecular dynamics simulations of aqueous 1,4-benzosemiquinone radical anion **1** as a prototype system, and to use the obtained trajectory data as input for DFT calculations of the electronic g-tensor of the system. This provides the first dynamical simulation of this important EPR parameter. The desired benefits from this ongoing project include a deeper knowledge of the dynamics of hydrogen bonding to semiquinone radical anions, and a detailed understanding of how intermolecular interactions influence the spectroscopic parameters from a dynamical point of view. Furthermore, we aim to produce accurate benchmark results, against which more approximate MD schemes (classical force field or combined quantum mechanics/molecular mechanics methods) may be validated in the future. Here, we provide results from about 6 ps of trajectory from a Car−Parrinello[19] ab initio molecular dynamics (CP-MD) simulation of benzosemiquinone in water, with an emphasis on hydrogen bonding dynamics. Moreover, we report first analyses of the dynamical effects of intermolecular interactions on the electronic g-tensor. Note that many of the more general results obtained here should also be transferable to other π-radicals in protic solvents.

Table 1. Dynamically Averaged g-Tensor Results (in ppm) for 150 Snapshots Taken from 1.0 ps of CP-MD Trajectory of Aqueous Benzosemiquinone Radical Anion

water molecules included	Δg_{iso}	Δg_x	Δg_y	Δg_z
d < 5.0 Å[a]	2684	4980	2912	162
d < 4.75 Å[a]	dev. +4[b]	dev. +9[b]	dev. +5[b]	dev. −1[b]
d < 4.5 Å[a]	dev. +23[b]	dev. +48[b]	dev. +17[b]	dev. +6[b]
d < 4.0 Å[a]	dev. +75[b]	dev. +157[b]	dev. +57[b]	dev. +12[b]
none	3822	8045	3334	90
H-bonds to O1[c]	3532	7318	3182	97
H-bonds to O2[c]	3496	7246	3160	83
H-bonds to O1 or O2[c]	2902	5560	3011	136
"T-stacking" H-bonds[c]	3931	8284	3406	105
all H-bonds[c]	2993	5716	3085	180
exp. (±50 ppm)[d]	2380	4180	2980	−20

[a] All water molecules within the given distance from any O or C atom of $BQ^{-\bullet}$ as specified in Methodological Details. [b] Deviation from the results for the largest clusters (d < 5.0 Å). [c] Small model clusters with only selected H-bond interactions in the first solvation shell. See Methodological Details section for H-bonding recognition criteria. [d] Cf. ref 47.

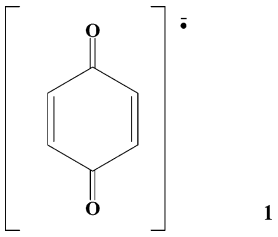

1

2. Methodological Details

CP-MD simulations[19] were performed using the CPMD program package (version 3.5.2)[20] on a system consisting of benzosemiquinone radical anion ($BQ^{-\bullet}$) and 60 water molecules in a periodically repeating unit cell of size 14.0 × 12.0 × 11.8 Å. We used the gradient-corrected BLYP density functional[21,22] in unrestricted open-shell Kohn−Sham calculations, with a plane-wave basis set truncated at 70.0 Ry, and Troullier−Martins norm-conserving pseudopotentials.[23] The electronic and nuclear equations of motion were integrated using a time step of 7 au (0.17 fs) and a fictitious electron mass of 1000 au. During an equilibration run of approximately 5 ps the temperature was set to an average of 300 K. The following 6.3 ps of trajectory were then used for analysis.

We have extracted 150 snapshots for g-tensor calculations from the final piece of trajectory, covering a time period of about 1 ps (that is, data were extracted every 6.8 fs or 40 time steps). From the extracted structural data, molecular cluster models were constructed and used in subsequent DFT g-tensor calculations. Initial test calculations (see Table 1) suggest that the g-tensor results are essentially converged with respect to cluster size to about 50 ppm in the largest component (Δg_x) when including in the calculation all water molecules with one or more atoms within 4.5 Å of a carbon or oxygen atom of the semiquinone, giving solvent clusters of 29−36 water molecules. While benzosemiquinone/water clusters obtained with this distance criterion are the basis for our ongoing investigations of EPR parameters in the system, the g-tensor calculations presented later in this paper were done with a larger 5.0 Å cutoff (corresponding to clusters including 37−45 water molecules;

(14) Nilsson, J. A.; Eriksson, L. A.; Laaksoonen, A. *Mol. Phys.* **2001**, *99*, 247.
(15) Nilsson, J. A.; Lyubartsev, A.; Eriksson, L. A.; Laaksoonen, A. *Mol. Phys.* **2001**, *99*, 1795.
(16) Raymond, K. S.; Grafton, A. K.; Wheeler, R. A. *J. Phys. Chem. B* **1997**, *101*, 623.
(17) Walden, S. E.; Wheeler, R. A. *J. Phys. Chem. B* **2002**, *106*, 3001. Grafton, A. K.; Wheeler, R. A. *J. Phys. Chem. B* **1999**, *103*, 5380. Zachariae, U.; Lancaster, R. D. *Biochim. Biophys. Acta* **2001**, *1505*, 280.
(18) DFT calculations with the BP86 functional reproduce the MP2 optimized structures of ref 8 to within 0.05 Å in the H-bond distances and to within a few kJ mol^{-1} in binding energies (after counterpoise corrections). This suggests a largely electrostatic nature of the interaction and very little dispersion character, in contrast to the π-stacked complexes between neutral quinones and indole.[8]
(19) Car, R. Parrinello, M. *Phys. Rev. Lett.* **1985**, *55*, 2471; Marx, D.; Hutter, J. In *Modern Methods and Algorithms of Quantum Chemistry*; Grotendorst, J., Ed.; NIC: Jülich 2000. (For downloads, see: www.theochem.rub.de/go/cvprev.html.)
(20) CPMD 3.5.2: Hutter, J.; Alavi, A.; Deutsch, T.; Bernasconi, M.; Goedecker, S.; Marx, D.; Tuckerman, M.; Parrinello, M. MPI für Festkörperforschung, Stuttgart and IBM Zurich Research Laboratory.
(21) Becke, A. D. *Phys. Rev. A* **1988**, *38*, 3098.
(22) Lee, C.; Yang, W.; Parr, G. R. *Phys. Rev. B* **1988**, *37*, 785.
(23) Troullier, N.; Martins, J. L. *Phys. Rev. B* **1991**, 43, 1993.

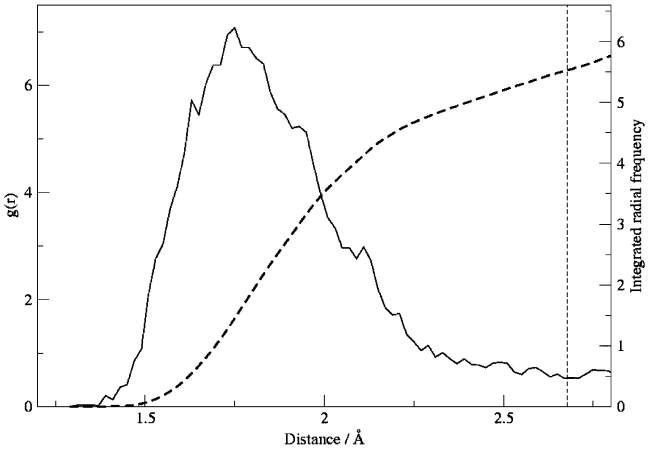

Figure 1. Radial distribution function for water proton/carbonyl oxygen OH···OC H-bonding distances, with integrated curve (dashed line) representing the number of water molecules found inside a given distance. Vertical dashed line shows minimum of RDF. Cf. Methodological Details section for the angle criteria employed.

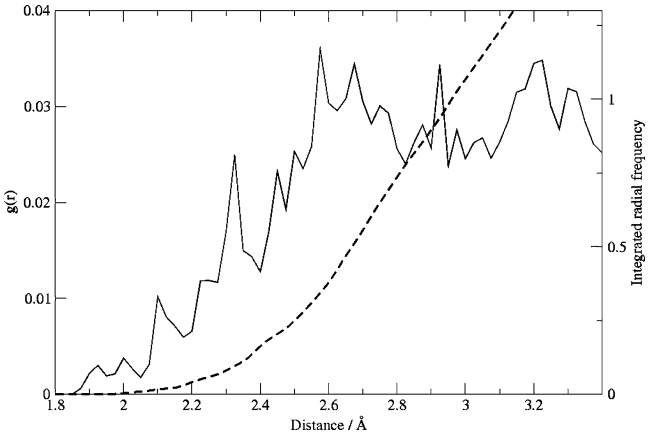

Figure 2. Radial distribution function for water proton/π-system (T-stacking) H-bonding OH···C distances, with integrated radial frequency curve (dashed line) representing the number of water molecules found inside a given distance. Cf. Methodological Details section for the angle criteria employed.

see Figure 3a for an example). For further analyses, calculations for the same snapshots from the CP-MD trajectory were additionally carried out for (a) the "naked" semiquinone, without any coordinated water molecules (but including any structural effects caused by the intermolecular interactions and intramolecular motion on the g-tensor), and (b) smaller cluster models including only specific interactions within the first solvation shell (either regular hydrogen bonds to the $BQ^{-\bullet}$ oxygen atoms, or T-stacked hydrogen bonds to the π-system, or both).

The electronic structure calculations for the cluster models were performed at the RIDFT level, using the gradient-corrected BP86 functional[21,24] and a DZVP Gaussian-type-orbital basis set[25] (SVP auxiliary basis sets[26] were used to fit the electron density). These unrestricted Kohn−Sham calculations employed the TURBOMOLE program (version 5.6)[27] and used tight SCF convergence criteria (energy 10^{-9} a.u., density 0.5×10^{-8} a.u.). Kohn−Sham molecular orbital (MO) information from the converged RIDFT calculations was transferred

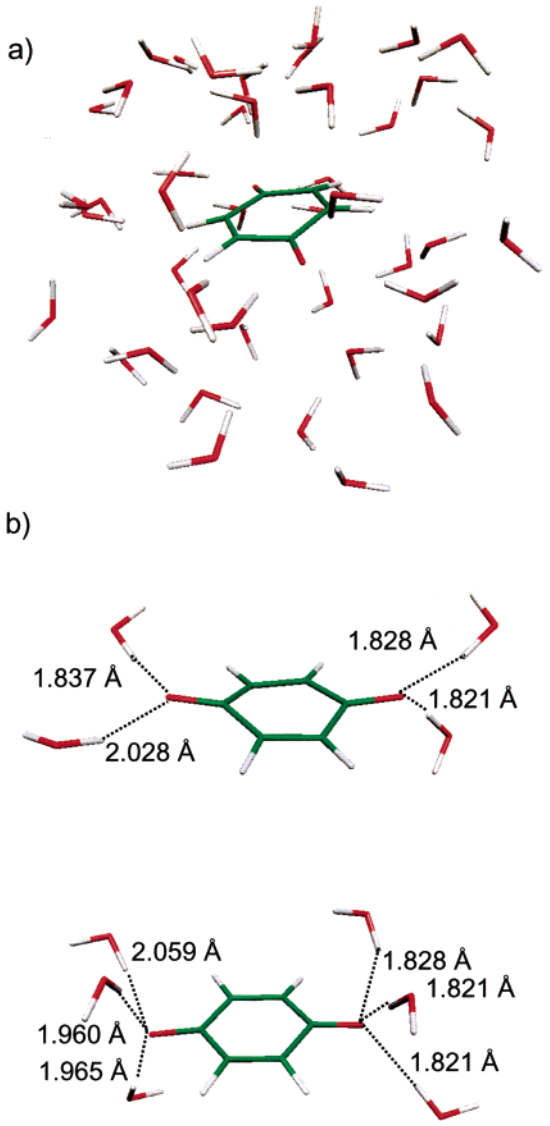

Figure 3. (a) Benzosemiquinone and all water molecules within a 5 Å distance criterion. This is an example cluster for an arbitrary snapshot from the CPMD trajectory. (b) Two representative examples of strongly out-of-plane hydrogen bonds to the carbonyl oxygen atoms. Only the semiquinone radical anion and those water molecules fitting the criteria of hydrogen bonds to the carbonyl oxygen atoms (four and five molecules, respectively) are shown. Distances in Å.

by recently constructed[4b] interface routines to the MAG (magnetic resonance) property module of the in-house program ReSpect.[28] The g-tensor calculations with MAG used the second-order perturbation theory ansatz of ref 4, including the dominant spin−orbit/orbital-Zeeman cross term $\Delta g_{SO/OZ}$ (eq 1), as well as the relativistic mass correction Δg_{RMC} and the one-electron part of the spin−orbit gauge-correction term Δg_{GC}.

$$\Delta g_{SO/OZ,uv} = \frac{g_e \alpha^2}{2S}\left[\sum_n \frac{\langle \Psi_0^{(0)}|H_{SO,v}|\Psi_n^{(0)}\rangle\langle \Psi_n^{(0)}|H_{oz}|\Psi_0^{(0)}\rangle}{E_0^{(0)} - E_n^{(0)}} + \text{c.c}\right] \quad (1)$$

In eq 1 (which is in atomic units), α denotes the fine structure constant, u and v are Cartesian coordinates, $\Psi_n^{(0)}$ the unperturbed ground-state

(24) Perdew, J. P.; Wang, Y. *Phys. Rev. B* **1986**, *33*, 8822. Perdew, J. P.; Wang, Y. *Phys. Rev. B* **1986**, *34*, 7406.
(25) Godbout, N.; Salahub, D. R.; Andzelm, J.; Wimmer, E. *Can. J. Chem.* **1992**, *70*, 560.
(26) Eichkorn, K. Treutler, O. Öhm, H. Häser, M. Ahlrichs, R. *Chem. Phys. Lett.* **1995**, *242*, 652.
(27) Ahlrichs, R.; Bär, M.; Häser, M.; Horn, H.; Kölmel, C. *Chem. Phys. Lett.* **1989**, *162*, 165. See also: Ahlrichs, R.; von Arnim, M. In *Methods and Techniques in Computational Chemistry: METECC-95*; Clementi, E., Corongiu, G., Eds.; Club Européen MOTECC, 1995, Chapter 13, pp 509ff.
(28) Malkin, V. G.; Malkina, O. L.; Reviakine, R.; Arbuznikov, A. V.; Kaupp, M.; Schimmelpfennig, B.; Malkin, I.; Helgaker, T.; Ruud, K. MAG-ReSpect (Version 1.1), 2003.

Table 2. Average Number of Hydrogen Bonds Found with Varying Distance Criteria[a]

H-bonds to carbonyl oxygen atom		T-stacked H-bonds	
distance cutoff (in Å)	average no.	distance cutoff (in Å)	average no.
2.0	3.5	2.6	0.46
2.1	4.0	2.8	0.80
2.2	4.5	3.0	1.11
2.3	4.8	3.2	1.44
2.4	5.0	3.4	1.82
2.5	5.2	3.6	2.25
2.6	5.4		
2.7	5.6[b]		

[a] Cf. Methodological Details for angular selection criteria. [b] First minimum of RDF, cf. Figure 1.

wave function, and $\Psi_n^{(0)}$ the unperturbed wave function of the *n*'th excited state (with eigenenergies $E_0^{(0)}$ and $E_n^{(0)}$ and, respectively). H_{SO} is the one- and two-electron spin−orbit operator, and H_{OZ} represents the orbital Zeeman term arising from the external magnetic field. The accurate and efficient atomic meanfield (AMFI) approximation[29,30] was used to compute the spin−orbit matrix elements. As was shown previously, this approach provides the currently most accurate quantum chemical results available for calculations of electronic g-tensors of bioradicals.[4−10,31] However, due to deficiencies in available gradient-corrected functionals such as BP86, we expect the largest g-shift tensor component, Δg_x, of π-radicals such as semiquinones to be overestimated by ca. 10% (we report g-shift components Δg_i—deviations from the free-electron value $g_e = 2.002\,319$—in ppm).[5,6,31] This may be corrected by suitable scaling (not performed here). A common gauge origin for the vector potential of the external magnetic field was used, located halfway between the two benzosemiquinone oxygen atoms (this is expected to be close to the center of spin density).

For the purpose of statistical analyses, and for the construction of small cluster models with specific, limited intermolecular interactions, we had to define suitable criteria for the presence or absence of hydrogen bonding in the first solvation shell. This was done as follows. A water molecule is considered H-bonded to a $BQ^{-\bullet}$ oxygen atom if either hydrogen fulfils the criteria R[H···O] ≤ 2.25 Å and <[O−H···O] ≥ 90°. Criteria for H-bonding to the π-system are: R[H···C] ≤ 3.0 Å, R[H···C] ≤ R[H···O], <[O−H···C] ≥ 120°, and <[H···C···m] ≤ 135° (*m* = center of mass of $BQ^{-\bullet}$). However, we have considered also a range of distance criteria, as shown in Table 2. We have plotted radial distribution functions *g*(r) (RDFs) for water molecules meeting the angular criteria in Figures 1 and 2 above. For the case of H-bonding to the π-system, certain approximations were made to obtain the RDF (detailed in Supporting Information). Figure 2 should thus be taken as indicative rather than definitive.

To obtain information about the energetics of T-stacked hydrogen bonding, we have in addition carried out a relaxed scan of the hydrogen-bonding potential energy curve for a small molecular model system involving the $BQ^{-\bullet}$ radical anion and one water molecule. These constrained optimizations were done at the unrestricted DFT level with the BP86 functional and DZVP basis sets, using the Gaussian 98 program.[32] We started from a fully optimized structure[8] of a complex of $BQ^{-\bullet}$ with an *N*-methylformamide (NMF) molecule. The NMF molecule was replaced at the same position by a water molecule, in which the H-bonded hydrogen was kept at the position above the ring located for the $BQ^{-\bullet}$(NMF) complex, but the H-ring distance was varied stepwise. The OH bond to this hydrogen atom was furthermore constrained to remain perpendicular to the ring (to avoid H-bonding between the second water hydrogen atom and the ring, which is unlikely in solution), but all other degrees of freedom were relaxed. Binding energies are reported after counterpoise correction[33] for basis-set superposition errors.

3. Results and Discussion

3.1. CP-MD Trajectory: Analysis of the Structural Dynamics of Hydrogen Bonding. The CP-MD trajectory provides important information, both on the intramolecular dynamics of the semiquinone, and on the dynamics of solvation. Here, we will concentrate on the latter and postpone the analysis of the former to a separate publication, in which also the analysis of the g-tensor results will be extended.[34]

Hydrogen Bonding to Carbonyl Oxygen Atoms. We find, as expected, extensive hydrogen bonding to the carbonyl groups of the benzosemiquinone radical anion. Using the criteria described in Section 2, we find between one and three hydrogen bonds to each carbonyl oxygen at almost any given time (very occasionally zero or four). The radial distribution of H-bonded water molecules has a maximum at around 1.75 Å (Figure 1),[35] with the shortest observed approach to $BQ^{-\bullet}$ being 1.32 Å. The latter, very short distances are already significantly on the repulsive part of the interaction, whereas the maximum of the RDF corresponds nicely to optimized distances in static calculations on suitable complexes between $BQ^{-\bullet}$ and water molecules.[5,11,13,36,37] We note that, although the energetically optimum position for hydrogen bonds is in the plane of the ring,[5] out-of-plane hydrogen bonds are also frequently observed in the simulation (see Figure 3b for examples). The RDF drops to a minimum at around 2.7 Å, which we consider as the separation between first and second solvation shells. Taking this as the cutoff distance, we find ca. 5.6 hydrogen bonds in the first solvent shell, that is 2.8 for each of the two carbonyl oxygen atoms, a relatively large number. We may compare our results to those of classical MD simulations: Raymond et al.[16] obtained an unrealistically short average hydrogen bond length of 1.6 Å for aqueous benzosemiquinone, and an average number of 3.3 hydrogen bonds per carbonyl oxygen atom. Longer average H-bond lengths of 1.75 and 1.77 Å and much lower average numbers of hydrogen bonds per oxygen of ca. 1.4 and 1.2 were found in recent simulations for models of aqueous plastosemiquinone[14] and ubisemiquinone,[15] respectively. Although a small part of the differences reflects steric effects for substituted

(29) Hess, B. A.; Marian, C. M.; Wahlgren, U.; Gropen, O. *Chem. Phys. Lett.* **1996,** *251*, 365.
(30) Schimmelpfennig, B. 1996 Atomic Spin−Orbit Mean-Field Integral Program, Stockholms Universitet, Stockholm, Sweden.
(31) *Ab initio and Density Functional Calculations of Electronic g-Tensors for Organic Radicals* Kaupp, M. in: *EPR Spectroscopy of Free Radicals in Solids. Trends in Methods and Applications*; Lund, A., Shiotani, M., Eds.; Kluwer: Dordrecht, 2003.
(32) Frisch, M. J.; Trucks, G. W.; Schlegel, H. B.; Scuseria, G. E.; Robb, M. A.; Cheeseman, J. R.; Zakrzewski, V. G.; Montgomery, J. A., Jr.; Stratmann, R. E.; Burant, J. C.; Dapprich, S.; Millam, J. M.; Daniels, A. D.; Kudin, K. N.; Strain, M. C.; Farkas, O.; Tomasi, J.; Barone, V.; Cossi, M.; Cammi, R.; Mennucci, B.; Pomelli, C.; Adamo, C.; Clifford, S.; Ochterski, J.; Petersson, G. A.; Ayala, P. Y.; Cui, Q.; Morokuma, K.; Malick, D. K.; Rabuck, A. D.; Raghavachari, K.; Foresman, J. B.; Cioslowski, J.; Ortiz, J. V.; Baboul, A. G.; Stefanov, B. B.; Liu, G.; Liashenko, A.; Piskorz, P.; Komaromi, I.; Gomperts, R.; Martin, R. L.; Fox, D. J.; Keith, T.; Al-Laham, M. A.; Peng, C. Y.; Nanayakkara, A.; Gonzalez, C.; Challacombe, M.; Gill, P. M. W.; Johnson, B.; Chen, W.; Wong, M. W.; Andres, J. L.; Gonzalez, C.; Head-Gordon, M.; Replogle, E. S.; Pople, J. A. *Gaussian 98, Revisions A.7, A.9*; Gaussian, Inc.: Pittsburgh, PA, 1998.
(33) Boys, S. F.; Bernardi, F. *Mol. Phys.* **1970**, *19*, 553.
(34) Asher, J. R.; Doltsinis, N. L.; Kaupp, M., unpublished results.
(35) That this RDF has a maximum value over twice that seen in ref 16 arises largely from a difference in definition: that work shows the RDF for all water hydrogen atoms, ours the RDF for all water hydrogen atoms H-bonded to a carbonyl group.
(36) Zhan, C.-G.; Chipman, D. M. *J. Phys. Chem. A* **1998**, *102*, 1230.
(37) Manojkumar, T. K.; Choi, H. S.; Tarakeshwar, P.; Kim, K. S. *J. Chem. Phys.* **2003**, *118*, 8681.

semiquinones,[5] the previous MD simulation results[16] on aqueous $BQ^{-\bullet}$ suffered clearly from too little repulsion of the potential at short distances (whereas the very low average numbers of hydrogen bonds in the substituted semiquinone simulations also appear unrealistic). The very accurate redox potentials for the $BQ/BQ^{-\bullet}$ system reported by the authors of ref 16 is thus expected to be based on severe error cancellation (possibly between intermolecular interactions of the different redox states, and the gas-phase DFT values used). We currently perform CP-MD simulations on the neutral system as well, to obtain a realistic description of the solvation for both redox states.[34] We note in passing that we expect the first maximum of $g(r)$ to be largely comparable to that obtained in ref 16 (also measured from carbonyl oxygen atoms), but the second to differ appreciably: the angular criterion applied here excludes solvent molecules above and below the π-system, the first solvation shell of which would start to contribute significantly to the O···H hydrogen-bonding RDF at about 3 Å. However, the most notable result here, the large average number of H-bonds, would not be affected by these criteria.

We also note that the mean carbonyl C−O bond length computed here is 1.303 Å, in reasonable agreement with the value of 1.31 Å inferred from vibrational data of aqueous benzosemiquinone,[38] significantly longer than the corresponding values in aprotic solvents (estimated 1.28 Å in DMSO[42]). Detailed analyses of intramolecular vibrations, and of their influence on the electronic g-tensor will be reported elsewhere.[34]

T-Stacked Hydrogen Bonding. In ref 8, we found from static quantum chemical calculations that a T-stacked hydrogen bond from a tryptophan N−H function (modeled by an indole) to the π-system of a semiquinone radical anion provides an appreciable energetic stabilization of ca. 50 kJ mol^{-1}. This provided an explanation[8] for the reorientation of the semiquinone in the active site of photosystem I, in which the native phylloquinone had been replaced by small quinones.[13] In contrast, the calculations showed that the neutral quinone prefers a π-stacked parallel arrangement with the tryptophan,[8] consistent with the X-ray structure of PS-I.[39] We argued that this type of redox-driven reorientation of semiquinone may also be a general feature of other quinone/semiquinone redox couples in biological systems.[8]

The model calculations in ref 8 also included a static optimization of a complex between $BQ^{-\bullet}$ and two perpendicular, T-stacked water molecules, and yielded a H···C distance of ca. 2.67 Å (in this case, each H_2O molecule had both hydrogen atoms pointing toward the ring carbons; T-stacked complexes of *N*-methyl-formamide exhibited the shortest H···C contacts near 2.45 Å). This suggests that T-stacking to the π-system of a semiquinone may also be present in protic solution.

Indeed, analysis of our CP-MD trajectory reveals appreciable T-stacked hydrogen bonds (see Figure 4 for a few representative structures). These are reasonably stable − lasting sometimes for hundreds of femtoseconds. The radial distribution function (Figure 2) for water molecules matching our T-stacking hydrogen-bond criteria (see above) exhibits a very broad

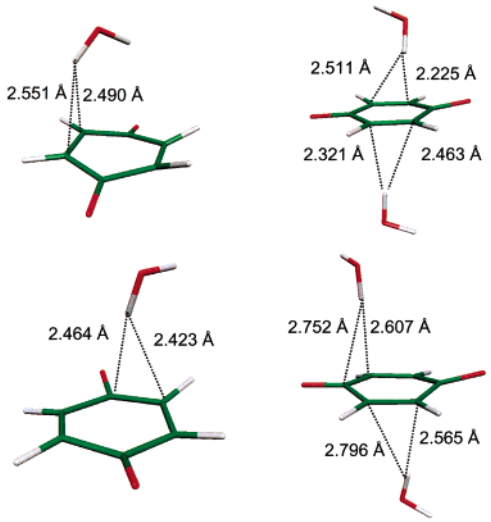

Figure 4. Representative examples of snapshots with T-stacked hydrogen bonds. Only the semiquinone radical anion and those water molecules fitting the criteria of T-stacked hydrogen bonds are shown. Distances in Å.

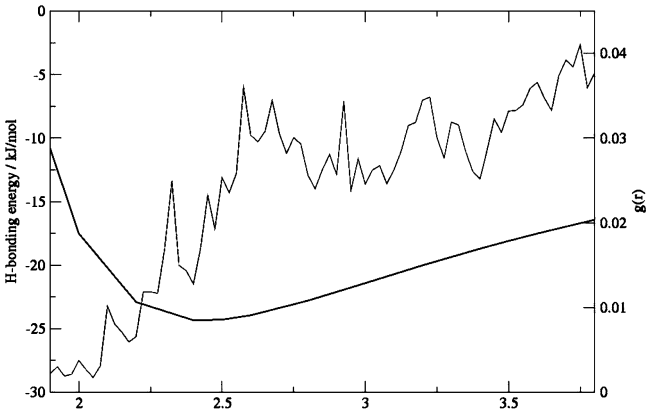

Figure 5. Potential well for single "T-stacked" hydrogen bond. Computed by a relaxed scan for a small molecular model complex (BP86/DZVP level, counterpoise-corrected; cf. Methodological Details). The dotted line represents the radial distribution function for the T-stacked hydrogen bonds from the CP-MD trajectory (cf. Figure 2).

maximum around 2.7 Å. It is difficult here to make out a distinct solvation shell, particularly as $g(r)$ does not go above 1.0, although the absolute values of $g(r)$ may not be reliable here. If instead we look at the number of water molecules fulfilling the $<[O-H\cdots C] \geq 120°$ criterion, as a proportion of the water molecules identified if this criterion is not imposed (measuring the degree to which water molecules are oriented toward the π-system at any given distance) we find that it is initially high and drops a little around 3 Å.

The shortest H-bonding distance observed is ca. 1.9 Å. We find a time average of 1.1 of these T-stacked hydrogen bonds below 3.0 Å (Table 2). Our static model calculations on a T-stacked $BQ^{-\bullet}(H_2O)$ complex (cf. Methodological Details) suggests the lowest energy near a hydrogen-ring distance of ca. 2.6 Å (cf. Figure 5; at this distance the hydrogen atom is about 2.45 Å above the ring; a 2.45 Å distance to the ring is also found if the hydrogen is forced to lie directly above a carbon atom). The counterpoise-corrected H-bond energy for this restrained model is ca. 19 kJ mol^{-1}, somewhat less than the ca. 50 kJ mol^{-1} computed for fully optimized T-stacked indole-semiquinone complexes[8] (a more realistic model for $BQ^{-\bullet}$−

(38) Knüpling, M.; Törring, J. T.; Un, S. *Chem. Phys.* **1997**, *219*, 291.
(39) Jordan, P.; Fromme, P.; Witt, H. T.; Klukas, O.; Saenger, W.; Krauss, N. *Nature* **2001**, *411*, 909.
(40) Kaupp, M., unpublished results.
(41) Zhao, X.; Kitagawa, T. *J. Raman Spectrosc.* **1998**, *29*, 773.
(42) Zhao, X.; Ogra, T.; Okamura, M.; Kitagawa, T. *J. Am. Chem. Soc.* **1997**, *119*, 5263.

H_2O interactions should provide binding energies between these two cases). In any case, the T-stacking is clearly also an intrinsic and important feature of the solvation of benzosemiquinone radical anion in water. We strongly suggest that this will generally be the case with semiquinones in protic solvents. Preliminary static model calculations suggest that the same holds also for phenolate anions,[40] and we expect that other negatively charged delocalized π-systems will exhibit similar interactions in protic solvents. The T-stacked hydrogen bonding to the π-system of such anions appears to be predominantly electrostatic in nature.[8]

In a recent resonance Raman spectroscopical investigation, Zhao and Kitagawa[41] suggested that the shift of the ν_{8a} vibrational mode of the semiquinone to higher frequency in protic solvents is due to T-stacked hydrogen bonds (a smaller effect in the same direction was noted for neutral BQ). Moreover, Zhao et al.[42] suggested that small differences between the Q_A and Q_B sites in bacterial photosynthetic reaction centers for the same mode might also arise from T-stacked interactions. However, this view has been criticized,[37] as the shift could already be reproduced by model clusters with only hydrogen bonds to the carbonyl oxygen atoms (partly due to mixing with a HOH bending mode in the water complex; see also ref 36). We cannot extract these types of small solvent-dependent shifts in vibrational frequencies from the current simulations. Static calculations on a small T-stacked BQ-•$(H_2O)_2$ model indicate a slight shift to *lower* frequency due to the T-stacked hydrogen bonds, which is expected to be overcompensated[36] by the effects of regular hydrogen bonding. Although some other modes are indeed shifted to higher frequencies, it will be very difficult to isolate the effects of the T-stacked interactions from the larger effects of regular hydrogen bonds (which may be in the same or in opposite direction for a given mode). It is thus unclear whether solvent effects on vibrational spectra of semiquinones can provide unambiguous evidence for T-stacked hydrogen bonding.

Indications for T-stacking may also be seen in the spatial distribution functions found in classical MD simulations for models of aqueous plastosemiquinone and ubisemiquinone, where distinct concentrations of hydrogen-atom density appear above certain ring atoms.[14,15] The energetic significance of these features appears to have gone unnoticed.

3.2. Preliminary Study of the Effect of Hydrogen Bonding on Electronic g-Tensor. Detailed EPR studies of semiquinone radical anions[2,3,43] (and of related π-radicals)[44] in different environments and static model calculations[5−7,9,45] have previously shown that hydrogen bonds to the semiquinone carbonyl oxygen atoms reduce significantly and characteristically the Δg_x component of the semiquinone. The Δg_y component is reduced moderately, whereas the Δg_z component is affected negligibly by in-plane hydrogen bonding. These observations are of great value in the determination of the environment of the bioradical under examination. This holds for semiquinones, tyrosyl radicals, or nitroxide spin labels alike and is based on the same principles. Initial interpretation was based on Stone's model,[46] which has been confirmed and refined by more quantitative calculations during the past decades. The reduction of g_x by hydrogen bonding is partly due to a lowering of the energy of the in-plane HOMO of the π-radical, which in all cases mentioned has substantial "lone-pair" character on the oxygen atom to which the hydrogen bond is formed (carbonyl oxygens for semiquinones or tyrosyls, the N−O oxygen in nitroxides). This enhances the energy gap entering the second-order perturbation expression (eq 1) for the $\Delta g_{SO/OZ}$ term.[7] Additionally, the spin density distribution of the π-radical is polarized by the hydrogen bond, removing some spin density from the oxygen and placing it on the neighboring atoms (in particular the ipso carbon atom in semiquinones and tyrosyls, the nitrogen atom in nitroxides).[5,7,38,43−45] The reduced spin density on the carbonyl oxygen atom (which has the largest spin−orbit coupling constant of the atoms in the system) also contributes to a reduction of g_x. The effect is much less pronounced for g_y, as this involves a lower-lying σ-type MO that is less modified by hydrogen bonding. The g_z component is not expected to be affected much, as it exhibits almost no noticeable $\Delta g_{SO/OZ}$ contributions under typical conditions and is thought to be dominated by Δg_{RMC} and Δg_{GC}. In contrast to the decrease in Δg_x and Δg_y by hydrogen bonding to the carbonyl oxygen atoms, our computational results[8] suggest that one T-stacked hydrogen bond to a semiquinone will *increase* both Δg_x and Δg_y by ca. 6−8%. We therefore expect counteracting effects from the two types of hydrogen bonding, with the "normal" hydrogen bonds to the carbonyl oxygens providing the dominant contribution.

With this previous experimental and static quantum chemical work in the field in mind, we report here the first molecular dynamics study of intermolecular effects on the g-tensor of a π-radical in protic solution, based on ca. 150 snapshots along 1.0 (out of 6.3) ps of the CP-MD trajectory of aqueous benzosemiquinone. A full analysis of a longer simulation will be reported in due course.[34]

Table 1 shows a summary of average results of a number of snapshot calculations. These calculations were done either on the large clusters with a cutoff radius up to 5.0 Å (37−45 water molecules; see Methodological Details), for "naked" $BQ^{-\bullet}$, or with small clusters in which only specific water molecules are included that give rise to the dominant solvation effects on the g-tensor. As expected, hydrogen bonding to carbonyl oxygens decreases Δg_x. The total effect in the presence of hydrogen bonds to both carbonyl groups is larger than the sum of the effects of hydrogen bonds to only one of the two groups. This is consistent with the analyses of static calculations in refs 5,6, which showed that single-sided hydrogen bonding leads to an asymmetric polarization of the spin density within the semiquinone toward the noncoordinated carbonyl oxygen atom, and thus to a less pronounced reduction of Δg_x. Comparison between small clusters and the larger clusters suggests that the direct hydrogen bond interactions of the carbonyl oxygen atoms with the first solvation shell account for approximately 75−80% of the overall decrease in Δg_x. The remaining 20−25% may be

(43) Zandstra, P. J. *J. Chem. Phys.* **1964**, *41*, 3655. Hales, B. J. *J. Am. Chem. Soc.* **1975**, *97*, 5993. Burghaus, O.; Plato, M.; Rohrer, M.; Möbius, K.; MacMillan, F.; Lubitz, W. *J. Phys. Chem.* **1993**, *97*, 7639. Rohrer, M.; Plato, M.; MacMillan, F.; Grishin, Y.; Lubitz, W.; Möbius, K. *J. Magn. Reson.* **1995**, *116*, 59. Nimz, O.; Lendzian, F.; Boullais, C.; Lubitz, W. *Appl. Magn. Reson.* **1998**, *14*, 255. Yonezawa, T.; Kawamura, T.; Ushio, M.; Nakao, Y. *Bull. Chem. Soc. Jpn.* **1970**, *43*, 1022.

(44) Un, S.; Atta, M.; Fontecave, M.; Brunel, L.; Rutherford, A. W. *J. Am. Chem. Soc.* **1995**, *117*, 10 713.

(45) See, e.g.: Törring, J. T.; Un, S.; Knüpling, M.; Plato, M.; Möbius, K. *J. Chem. Phys.* **1997**, *107*, 3905. Knüpling, M.; Törring, J. T.; Un, S. *Chem. Phys.* **1996**, *219*, 291. See also: Engström, M.; Vaara, J.; Schimmelpfennig, B.; Ågren, H. *J. Phys. Chem. B* **2002**, *106*, 12 354.

(46) Stone, A. J. *Proc. R. Soc. A* **1963**, *271*, 424. Stone, A. J. *Mol. Phys.* **1964**, *6*, 316.

due to polarization of the water molecules in the first solvation shell by their further interactions with the next shell, or due to direct long-range electrostatic interactions (note that calculations with a polarizable continuum model provide only relatively small long-range effects on g_x[7]). The overall reduction of Δg_x by hydrogen bonding in the large cluster calculations is close to 40% relative to the "naked" semiquinone results for the same snapshots (Table 1). In contrast, the reduction of Δg_y is only ca. 10−12%. Notably, Δg_z is increased by ca. 73 ppm, that is, by almost 80%! This effect is already complete with only the direct hydrogen bonds to the carbonyl oxygen atoms present. Closer inspection indicates that occasional hydrogen bonds with strong out-of-plane character make small but notable $\Delta g_{SO/OZ}$ contributions to Δg_z.

Our study in ref 8 suggested that a T-stacking hydrogen bond increases both Δg_x and Δg_y. This is confirmed by the average results in Table 1, which indicate an enhancement of Δg_x by ca. 4% and of Δg_y by ca. 2%. Given that analysis of these snapshots suggests about 1.0 T-stacked hydrogen bond interactions below a cutoff of 3.0 Å, these results are consistent with the increase of ca. 8% found for both components in static calculations on suitable T-stacked complexes:[8] in those, hydrogen-bond lengths of ca. 2.35−2.45 Å are found, whereas the radial distribution function of our trajectory shows its highest value at around 2.7 Å. Overall, the calculations show clearly that the effect of the T-stacked hydrogen bonds on the g-tensor is counteracted by opposite, and much larger, effects from the other hydrogen bonds. Nevertheless, a reliable prediction of the g-tensor has to take the T-stacking into account.

In a recent Q-band EPR and ENDOR study, Flores et al.[47] provided the first g-tensor data of $BQ^{-\bullet}$ in water at 80 K (isotropic g-values in liquid water at 300 K have been known for a long time[43a]). Our number of snapshots may be insufficient at this stage to allow a reliable comparison of statistical average values with experiment. Table 1 includes the data of Flores et al. nevertheless. We immediately see that our preliminary simulation result for Δg_y is in reasonable agreement with experiment, whereas Δg_x is about 24% high. A ca. 8−10% overestimate has already been inferred from previous static calculations and was attributed to systematic deficiencies of the gradient-corrected density functional employed in describing the dominant HOMO−SOMO contribution to Δg_x.[5] A systematic scaling of static calculation results on supermolecular semiquinone/2-propanol model complexes by a factor of 0.92 of Δg_x gave excellent agreement with experimental data for a range of semiquinones in frozen 2-propanol solution.[5] Part of the larger discrepancy in the present work on aqueous benzosemiquinone radical anion is due to slightly improved Kohn−Sham orbitals: In ref 5, the Kohn−Sham-SCF calculations used the deMon program and involved a fitting of both charge density and exchange-correlation potential by auxiliary basis sets. The present calculations with the TURBOMOLE program use fitting only for the charge density, with somewhat larger auxiliary basis sets. Test calculations indicate that this increases Δg_x by ca. 3% compared to the deMon results. Rather than the scaling factor of 0.92 proposed,[5,6,8] a scaling factor of ca. 0.89 appears thus to be more appropriate in comparing the present RIBP86 results with experiment. This leaves us still with an overestimate of ca. 6% of Δg_x by our current, preliminary simulation results. This may well change when a larger fraction of the trajectory has been sampled. On the other hand, deviations on this order of magnitude may already be caused by the approximations inherent in the cluster model. Interestingly, this slight overestimate of Δg_x is obtained irrespective of the fact that our simulations indicate an unexpectedly high average number of hydrogen bonds. This gives us additional confidence in our simulation results.

The relatively narrow ENDOR lines in ref 47 for those water hydrogen atoms hydrogen-bonded to the semiquinone oxygens have been suggested to indicate a narrow distribution of hydrogen-bond distances. This contrasts with our relatively broad RDF in Figure 1. To obtain a preliminary estimate of ENDOR line widths, we have computed hyperfine coupling (HFC) tensors for our small static $BQ^{-\bullet}(H_2O)$ model as a function of H-bond lengths (at B3LYP/EPR−II level; data not shown). Convoluting the computed A_z component of the HFC tensor with the RDF of Figure 1, we obtain an average of 6.48 MHz and a half-width at half-maximum of ca. 1.9 MHz. Comparing this to an experimental value of 6.36 MHz and a line width of ca. 0.3 MHz suggests that the ENDOR experiments in frozen solution at 80 K do indeed sample a much smaller coordinate space of hydrogen bond lengths than our simulations in the liquid phase at 300 K. We are currently computing hyperfine tensors directly for the same snapshots and cluster models used in the g-tensor computations, to obtain a more quantitative treatment.

4. Conclusions

As part of a continuing investigation, the present study has provided a wealth of information about the dynamics of hydrogen bonding to semiquinone radical anions in protic solution. The chosen model system, benzosemiquinone in aqueous solution, may be viewed as prototype, and many of our findings should be transferable to a variety of other systems—including, to some extent, protein environments. Most notably, the CP-MD simulations have identified not only a relatively large number of about 4−5.6 hydrogen bonds (on average) to the carbonyl oxygen atoms of the semiquinone, but also surprisingly long-lived T-stacked hydrogen bonds to the π-system of the semiquinone radical anion. This confirms conclusions from recent computational studies on the A_1 site of photosystem I:[8] T-stacked hydrogen bonding to the π-system of semiquinone radical anions, and most likely to other related negatively charged delocalized π-systems, is an appreciable interaction that exceeds known T-stackings to neutral aromatic systems such as benzene[48] by at least a factor of 3 in stability. These novel interactions may furthermore be expected to appreciably affect redox potentials involving such anions.

The preliminary g-tensor results provided here represent the first dynamical simulation of this EPR parameter from quantum chemical calculations. While the simulations confirm the conclusions from previous static calculations concerning the effects of normal and of T-stacked hydrogen bonds on the g-tensor components of semiquinone radical anions, they provide a much more detailed picture than available before. We see, for example, that the direct hydrogen bonds to the semiquinone

(47) Flores, M.; Isaacson, R. A.; Calvo, R.; Feher, G.; Lubitz, W. *Chem. Phys.* **2003**, *294*, 401.

(48) See, e.g.: Chipot, C.; Jaffe, R.; Maigret, B.; Pearlman, D. A.; Kollman, P. A. *J. Am. Chem. Soc.* **1996**, *118*, 11 217.

provide a large part but not all of the solvent effect on the g-tensor. Long-range effects of the next solvent shells appear to be nonnegligible. T-stacked hydrogen bonds to the semiquinone π-system provide a small but important contribution that is of opposite sign to those from the "normal" hydrogen bonds.

Our ongoing investigations include g-tensor snapshot calculations over a larger part of the 6.3 ps CP-MD trajectory obtained. This should allow close analysis of intramolecular dynamics and of their influence on the g-tensors, as well as better statistics of the g-tensor dynamics. We currently investigate also dynamical effects on hyperfine couplings (see above), and we carry out simulations of neutral aqueous benzoquinone, to obtain estimates of dynamics and solvation on the important redox potentials of quinone/semiquinone redox couples.[34] The present data should furthermore serve to calibrate force fields for classical or mixed classical/quantum-mechanical MD simulations.

Acknowledgment. We are grateful to D. Marx (Bochum) for insightful discussions and partial support and A. V. Arbuznikov (Würzburg) for additional discussions. This study has been funded by Deutsche Forschungsgemeinschaft within the Priority Program SP1051 on "High-Field EPR Spectroscopy in Chemistry, Biology, and Physics" (KA1187/4). J.R.A. acknowledges a scholarship within the graduate college "Electron Density" at Universität Würzburg. The CP-MD simulations were carried out at the Leibniz Rechenzentrum in München on the SR8000-F1 Bundeshöchstleistungsrechner (HLRB project h0731). For the preparation of Figure S2 we thank Chris Page (Manchester University).

Supporting Information Available: An Appendix with three Figures (S1-S3) explains the derivation of radial distribution functions. This material is available free of charge via the Internet at http://pubs.acs.org.

JA0485053